The Spine Journal 19 (2019) 532–544

Basic Science

New evidence for structural integration across the cartilage-vertebral endplate junction and its relation to herniation

Nurul Haiza Sapiee, BEng[a], Ashvin Thambyah, PhD[a], Peter A. Robertson, MD[b], Neil D. Broom, PhD[a,*]

[a] *Experimental Tissue Mechanics Laboratory, Department of Chemical and Materials Engineering, The University of Auckland, 20 Symonds St, 1010 Auckland, New Zealand*

[b] *Department of Orthopaedic Surgery, Auckland City Hospital, 2 Park Road, 1023 Auckland, New Zealand*

Received 15 June 2018; revised 24 August 2018; accepted 27 August 2018

Abstract

BACKGROUND CONTEXT: The cartilaginous and bony material that can be present in herniated tissue suggests that failure can involve both cartilaginous and vertebral-endplates. How structural integration is achieved across the junction between these two distinct tissue regions via its fibril and mineral components is clearly relevant to the modes of endplate failure that occur.

PURPOSE: To understand how structural integration is achieved across the cartilaginous-vertebral endplate junction.

STUDY DESIGN: A micro- and fibril-level structural analysis of the cartilage-vertebral endplate region was carried out using healthy, mature ovine motion segments.

METHODS: Oblique vertebra-annulus-vertebra samples were prepared such that alternate layers of lamellar fibers extended from vertebra to vertebra. The endplate region of each sample was then decalcified in a targeted manner before being loaded in tension along the fiber direction to achieve incomplete rupture within the region of the endplate. The failure regions were then analyzed with differential interference contrast microscopy and scanning electron microscopy.

RESULTS: Microstructural analysis revealed that failure within the endplate region was not confined to the cement line. Instead, rupture continued into the underlying vertebral endplate with bony material still attached to the now unanchored annular bundles. Ultrastructural analysis of the partially ruptured regions of the cement line revealed clear evidence of blending/interweaving relationships between the fibrils of the annular bundles, the calcified cartilage and the bone with no one pattern of association appearing dominant. These findings suggest that fibril-based structural cohesion exists across the cement line at the site of annular insertion, with strengthening via a mechanism somewhat analogous to steel-reinforced concrete. The fibrils are brought into a close intermingling association with interfibril forces mediated via the mineral component.

CONCLUSIONS: This study provides clear evidence of structural connectivity across the cartilaginous-vertebral endplate junction by the intermingling of their fibrillar components and mediated by the mineral phase. This is consistent with the clinical observation that in some disc herniations bony material can be still attached to the extruded soft tissue.

Keywords: Structural integration across CEP-VEP junction; Micro- and fibril-level structural analysis; Mechanism analogous to steel reinforced concrete; Relevance to herniation.

FDA device/drug status: Not applicable.

Author disclosures: ***NHS***: Grant: Medtronic Australasia (F NZD, doctoral stipend support). ***AT***: Nothing to disclose. ***PAR***: Educational Consultancy unrelated to this paper: Medtronic (B NZD, expense reimbursement), NuVasive B NZD, expense reimbursement), LifeHealthcare (B, expense reimbursement) ***NDB***: Grant: Medtronic Australasia (F NZD, doctoral stipend support).

The disclosure key can be found on the Table of Contents and at www.TheSpineJournalOnline.com.

* Corresponding author. Experimental Tissue Mechanics Laboratory, Department of Chemical and Materials Engineering, The University of Auckland, Private bag 92019, 20 Symonds St, 1010 Auckland, New Zealand. Tel.: (64)9-9238974; fax: (64) 9-3737463.

E-mail address: nd.broom@auckland.ac.nz (N.D. Broom).

https://doi.org/10.1016/j.spinee.2018.08.013

Introduction

Disc disruption and herniation are commonly associated with sciatica and low back pain [1–6], and in vivo studies have shown that lumbar disc herniation in humans is more commonly associated with endplate junction failure than with mid-substance annular rupture [3]. Such findings emphasize the importance of focusing on the endplate junction as a primary region of interest in disc herniation [3]. As further support for such a focus, Lama et al. [4] found fragments of cartilage or bone in about 50% of discs with extruded herniated matter, demonstrating modes of structural failure involving the endplate junction.

Employing magnetic resonance imaging (MRI), Sahoo et al. [5] showed that endplate lesions are commonly associated with symptomatic lumbar disc herniation and demonstrated the involvement of both cartilaginous endplate (CEP) and vertebral endplate (VEP). Questions therefore arise as to the causes of such region-specific failures in the disc-endplate complex. To address such a question requires a detailed ultrastructural exploration of this complex region, one involving three very different tissue matrices.

The CEP acts as an important structural transition between the compliant disc tissues and the rigid vertebral bone [6,7]. The tough annular fibers anchor in the cartilaginous endplate via the insertion of annular subbundles at the tidemark (TM) [6,7]. However, it remains less clear as to how integration is achieved across the CEP-VEP junction or cement line (CL).

Multiscale structural analysis has provided some evidence of short-range fibril integration at the CL in an ovine lumbar model [7] as well as for annular subbundles anchoring into the CEP, and then entering the VEP in human motion segments [8]. This supports an earlier suggestion by Humzah and Soames [9] that the annular fibers anchor not only into the CEP but also into the compact bony zone through an interwoven structure between the annular fibers and the bony fibril lamellae, thereby hinting at a structural basis for the potential strength of this region.

Using T10–L1 motion segments from human spines in the age range 49 to 65 years, Berg-Johansen et al. [10] reported that the CEP and VEP were not well-integrated in the inner annulus region. There is also little published evidence of collagen fibers crossing the junction between the CEP and VEP of human lumbar spines [11], which supports the view that it is a potentially weak link in the disc-endplate complex, thereby enabling the CEP to be stripped from the VEP [12]. Such findings are consistent with several other studies arguing either for an absence of interconnectivity between the CEP and VEP [13] or that it remains somewhat obscure [14].

However, we cannot ignore the fact that the CEP and VEP are mechanically well connected. Vernon-Roberts et al. [15] noted the normally “tight bonding” between the two regions in human motion segments, and Rodrigues et al. [7] demonstrated a similar robustness in ovine lumbar motion segments. And although it is generally accepted that the mineral phase in the cartilaginous endplate provides an important degree of reinforcement of this transition region [7,8,16–18], it remains much less clear as to whether there is some kind of intimate structural association between the fibrous elements and mineral phase as is the case in fiber-reinforced composite materials.

Employing an ovine lumbar spine model the aim of this new study was to investigate to what extent fibril-level structure could be involved in the creation of this mechanically robust junction between the CEP and VEP. Specifically, we have developed a technique that induces partial rupture of the CL as a means of investigating this question.

Materials and methods

Mature ovine lumbar spines from 2- to 4-year-old animals were obtained fresh from the slaughterhouse and stored at −20°C until required. Small oblique vertebra-annulus-vertebra samples (~5 × 5 mm in cross section) were sawn from the anterior and posterior aspects of the still frozen motion segments and in line with one of the oblique-counter oblique fiber directions, as illustrated in Fig. 1. This sample format was to enable an in-plane tension to be applied along the chosen oblique direction.

In order to provide test controls (ie, mechanically tested without any chemical treatment), eight samples were hydrated overnight in physiologic saline solution at 4°C before being extended axially at a rate of 0.05 mm/s up to the point of rupture. Three additional nontest control samples were subjected to energy-dispersive X-ray spectroscopic analysis using a scanning electron microscope (SEM) to measure the weight percentage change in mineralization across the disc-endplate region, targeting specifically calcium and phosphorous.

The vertebral bone ends of 49 other samples were then carefully coated with dental plaster to act as a water-proofing layer prior to being chemically fixed in 10% formalin to stabilize biologically the still uncoated regions of the samples. These samples were then placed in 10% formic acid for up to 56 hours, which allowed decalcification of the endplate region while still leaving the bulk of the vertebral bone fully mineralized so as to permit gripping during tensile loading. The in-plane annular span of each sample was measured and the dental plaster coating then removed prior to its tensile stretching at a rate of 0.05 mm/s. Each test was set to terminate at a 40% reduction in load; this is designed to induce partial rupture in the vicinity of the now decalcified CEP-VEP junction.

These samples were then further decalcified in order to obtain full in-plane 30-μm thick sections using cryosectioning (Fig. 1a). These sections were then examined fully hydrated using differential interference contrast (DIC) light

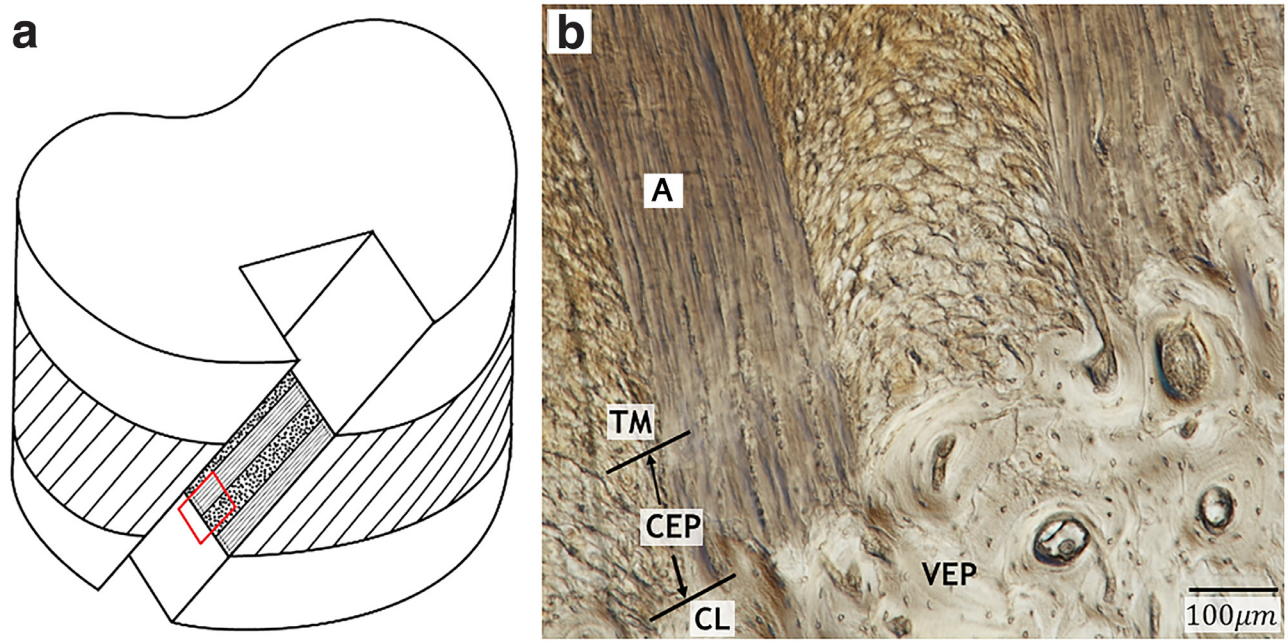

Fig. 1. (a) Schematic illustrating how vertebra-annulus-vertebra samples were obtained from the anterior aspect of the motion segment so as to incorporate in-plane, one of the oblique fiber sets that pass from endplate to endplate. Note that the red-boxed region identifies the endplate region of interest. (b) Optical DIC image of a fully hydrated in-plane thin section showing the annulus-endplate junction in the boxed region in (a). CEP, cartilaginous endplate; VEP, vertebral endplate; TM, tidemark (only faintly visible); CL, cement line; A, annulus.

microscopy (Fig. 1b). Selected sections were also critical point dried and then analyzed at the fibril level using SEM.

Of the 49 samples that were tested, 18 failed wholly within the vertebral bone distant from their endplates – these were discarded. The remaining 31 samples were successfully tested and then examined using DIC microscopy, of which 15 were further analyzed by SEM, with some involving multiple section analysis.

Results

General

For the eight test control samples, six failed in the mid-substance annulus (Fig. 2) and two within the gripped region of the vertebral bone proper, and because none failed in the region of the endplate, they were not subjected to any further structural analysis beyond this macrolevel observation. Energy-dispersive X-ray spectroscopic data for one of the three additional nontest control samples are shown positionally and quantitatively in Fig. 3 and Table 1, respectively. All three nontest control samples exhibited a similar sharp increase in both calcium and phosphorous in crossing the TM; this increase persisted through and beyond the CL.

All results pertaining to the formalin-fixed and decalcified samples reflect an unavoidable component of chemically induced artifact and thus preclude any direct mechanical comparison with the test controls. However, the chemical treatment did provide a means of investigating the influence of the tissue's mineral component in contributing to CEP-VEP junction strength (see later discussion of this issue).

Microlevel structural analysis

Differential interference contrast imaging determined where, in the vicinity of the endplate, rupture had occurred (Fig. 1b). Table 2 details the location of rupture within the endplate region for each of the 31 demineralized samples.

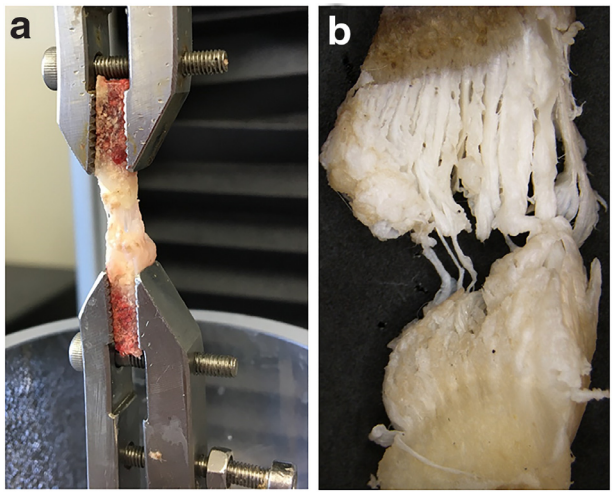

Fig. 2. (a) Image of a test control sample being subjected to tensile loading along direction of in-plane annular fibers. (b) Image showing how failure in the untreated samples mainly occurred within the mid-substance annular fibers.

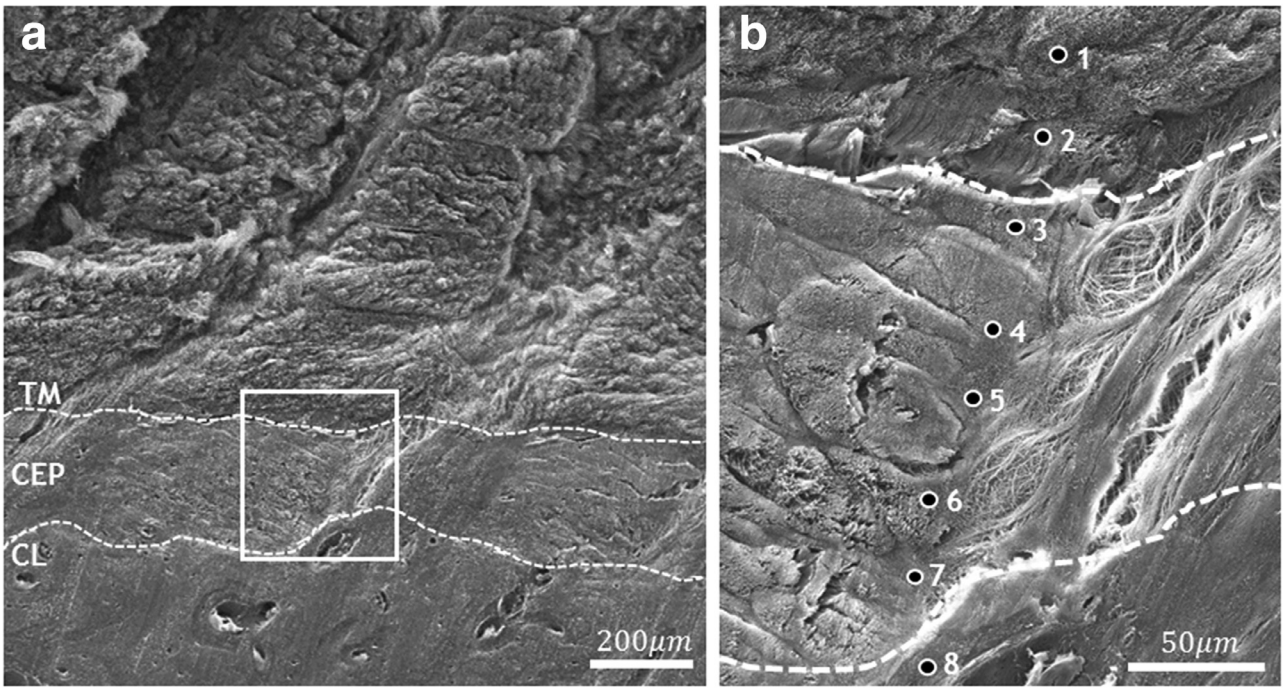

Fig. 3. (a) Low-magnification SEM image showing approximate locations of tidemark (TM), cartilaginous endplate (CEP), and cement line (CL) on one of the three nontest control samples subjected to energy-dispersive X-ray spectroscopic (EDX) analysis. (b) Enlarged view of boxed region in (a) showing the locations numbered from 1 to 8 across the TM and CL where EDX analysis was performed.

Interestingly, although only two samples failed within the mid-substance of the annulus, these also contained tears in the region of the endplate (see Fig. 8a). In some samples, rupture was confined to one endplate, the other end thus acting as an intact "control" for the chemically modified tissues. In other samples, both endplates were ruptured.

For all endplate failures, rupture commenced beneath the inner annulus followed by outwards radial propagation and tracked both along the CEP-VEP junction and within the VEP as is evident from the bony osteons still attached to the in-plane layers (Fig. 4). This inclusion of VEP material with the separation (see white arrow and dashed-box in Fig. 4a) suggests a significant degree of integration across the junction. The pull-out of the osteons even after removal of the mineral phases suggests an underlying structural connectivity independent of any strengthening provided by the mineral component.

Table 1
Showing the positional distribution and weight% of calcium (Ca) and phosphorous (P) in the nontest control sample illustrated in Fig. 3

	Weight%	
Region	Ca	P
1	1.21	0
2	7.27	1.92
3	32.37	21.90
4	36.21	24.50
5	28.27	16.62
6	35.65	21.91
7	29.21	17.75
8	47.39	27.21

Fibril-level structural analysis

Table 2 also details the approximate morphologies of integration at the fibril level. Although the enlarged microscopic view of the boxed region in Fig. 4 (a) hints at the annular subbundles extending into the VEP (see arrowed sites in Fig. 4b), it is only with SEM that we begin to see more clearly the nature of the structural integration across the CEP-VEP junction. In the image set in Fig. 5, we can trace the continuity of the annular subbundle fibrils within the CEP as they insert deep between the bony osteons of the VEP (Fig. 5a and b), and this is consistent with the DIC image in Fig. 4(b). We too note that the subbundle fibrils appear to end abruptly on meeting the osteon fibrils (Fig. 5c), although this may well be an artifact resulting from the plane of sectioning.

The SEM image sets in Figs. 6 to 9 reveal additional fibril-level morphologies which suggest a range of associations between the subbundle fibrils and osteons. For example, Fig. 6 illustrates a well-defined anchoring of fibril subbundles in the osteons and involving subbundles of widely varying diameters inserting into local regions of the VEP bone (cf. Fig. 6b and e). Further, some anchorage sites provide clear evidence of a near-aligned blending between the subbundle and osteon fibrils (Fig. 6c).

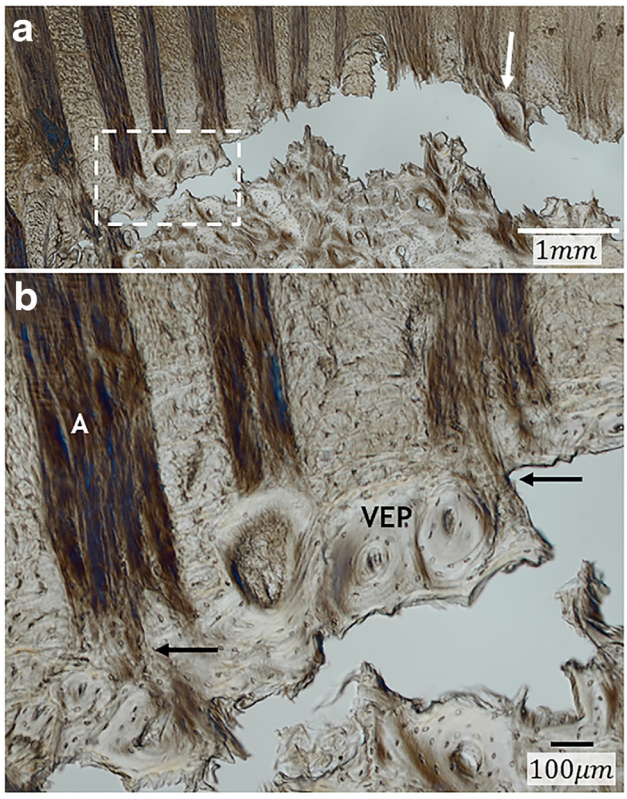

Fig. 4. (a) Representative optical DIC image of a sample failing in the endplate near the cement line (CL). The failure is seen to combine tears along the CL junction as well as within the VEP as shown by the presence of the bony osteons attached to the pulled out annulus (see sites identified by white arrow and boxed region). (b) Enlarged view of boxed region in (a) and showing portions of VEP still attached to the pulled out annular bundles. Note also at sites marked by the black arrows, some annular fibers appear to extend into the VEP.

Another mode of integration illustrated in the set of images in Fig. 7 appears to involve an array of less organized bony fibrils that could be interpreted as providing a mediating link between the aligned annular subbundles and the highly structured osteon layers (Fig. 7a). This mode of integration also included more organized bony fibrils located between the annular subbundles near the junction and thus hinting at a localized pattern of interdigitation (Fig. 7b).

In those samples that suffered both mid-substance annular rupture and partial tearing along the CEP-VEP junction, there was also evidence of bony osteons remaining attached to the pulled-out annular layers (see arrows in the DIC image in Fig. 8a). The still intact boxed region in Fig. 8a is shown enlarged with SEM imaging in Fig. 8b. This, together with the further enlargement in Fig. 8c, indicates a prerupture peeling away of the annular subbundles from those of the bony osteons, suggesting a close blending of the two structures.

Although infrequently observed, subbundle fibrils could also terminate abruptly without any obvious hint of merging with the osteon fibrils, giving the appearance of a slight physical separation or gap (Fig. 9d and possibly Fig. 5c). Such gaps appeared to extend only short distances in the plane of the endplate (Fig. 9d) before being replaced with structure indicating a more integrative relationship between subbundles and osteons (Fig. 9c).

The overall impression gained from the fibril-level analyses was that although the subbundle fibrils and osteon fibrils were closely associated in most regions of the CEP-VEP junction, no one morphology of integration appeared to dominate.

Discussion

The test control samples (ie, fully mineralized) subjected to the tensile testing regime employed in the present study invariably failed by mid-substance annular rupture or in the vertebral bone proper. This highlights the strength of the CEP-VEP junction relative to that of the annular tissue and confirms the assertion of Vernon-Roberts et al. [15] that there is normally tight bonding across this junction.

It is important to emphasize that fixing the entire vertebra-annulus-vertebra samples and then locally decalcifying the endplate region *before* tensile loading up to the point of initial rupture has several consequences, some positive and others negative. The formalin fixation (required to render the tissues biologically stable during the extended period of decalcification), by virtue of its crosslinking action on the matrix proteins, will stiffen (and strengthen) considerably the previously highly compliant annular structures. It is likely that the CEP and VEP, being already mineralized, will be much less affected by this fixation, although there will be an increased crosslinking of their respective collagens.

The formic acid decalcification of the now fixed samples then strips out the mineral component in the endplate region, and any additional weakening influence it might have will likely apply to both the annulus and endplate tissues. Thus, although such a sequence of chemical treatments precludes any mechanical comparison with the fresh tissue response, we argue that our treated samples do offer a novel means of comparing the susceptibility to rupture of the different structural regions within a given sample. It must also be borne in mind that any inferences drawn concerning the mechanisms of endplate rupture relate only to those regions of the endplate that have been directly loaded by the annular layers whose fibers lie in-plane within our vertebra-annulus-vertebra samples. The near cross-sectioned annular layers alternating with the in-plane layers will carry no tensile loading in our samples and are therefore ignored.

The targeted 56-hour demineralization treatment employed in the present study contrasts with the total sample demineralization technique employed previously by Rodrigues et al. [6]. These investigators exposed the entire disc-vertebral segment to 14 days of formic acid treatment for the purposes of structural analysis only.

Table 2
Failure modes and ultrastructural morphologies of all samples that failed at the cement line (CL)

Motion segment	A/P	Failure modes			Ultrastructural morphology across CL				Illustrated in figure	# Sections observed under SEM
		Annular mid-subst	Both CLs	VEP attached	Fibrils extend deep in VEP	Fibrils anchor-ing	Fibrils inter-weaving	Fibrils termin-ating		
S1,L1L2	A		•	•		No ultrastructural analysis				
S1,L1L2	P			•		No ultrastructural analysis				
S1,L2L3	P			•		No ultrastructural analysis				
S1,L2L3	A			•	•	•				2
S1,L3L4	A			•	•		•			3
S2,L3L4	A			•	•	•				1
S3,TL1	A			•	•	•				2
S3,L1L2	A			•	•	•	•			3
S4,L1L2	A		•	•		No ultrastructural analysis				
S4,L2L3	A			•		No ultrastructural analysis				
S5,TL1	A	•		•	•	•	•		Fig. 5a-c; 6c,f,g; 7a; 8a-c	3
S5,TL1	P			•		No ultrastructural analysis				
S5,L1L2	A		•	•		•	•		Fig. 7b	3
S5,L2L3	A	•		•		No ultrastructural analysis				
S5,L2L3	P			•		No ultrastructural analysis				
S5,L4L5	A			•	•	•	•			1
S5,L5L6	A		•	•	•	•	•	•	Fig. 6a,b; 9a-d	5
S5,L5L6	P			•		•				1
S6,TL1	A			•		•	•	•		1
S6,TL1	P			•		No ultrastructural analysis				
S7,TL1	A		•	•	•	•	•		Fig. 4a,b; 6d,e	4
S7,TL1	P			•		No ultrastructural analysis				
S7,L1L2	P			•		No ultrastructural analysis				
S7,L2L3	A		•	•		No ultrastructural analysis				
S7,L2L3	P			•		No ultrastructural analysis				
S7,L3L4	P			•		No ultrastructural analysis				
S8,TL1	A			•		•				1
S8,L1L2	A			•			•			1
S8,L1L2	P			•		No ultrastructural analysis				
S8,L2L3	A		•	•		•				1
S8,L2L3	P			•		No ultrastructural analysis				
Total		2	7	31	9	13	9	2		32

A, Anterior; **P**, Posterior; • indicates yes.
Both CLs indicates failure at CL of both endplates; **VEP attached** indicates portions of the VEP were attached to the pulled-out subbundles.

The technique devised for the present study provided a targeted demineralization of the endplate region while leaving the bulk of vertebral bone largely mineralized and thus able to be gripped in the tensile testing machine. This technique enabled us to induce partial rupture along or close to the CEP-VEP junction in most samples. Such rupture behavior indicates that mineralization plays a key role in strengthening this critical junction. But equally, the fact that annular subbundle pull-out frequently included portions of the VEP suggests that even in its demineralized state there remains a sufficient level of interconnectivity between the fibrils of the CEP and VEP independent of the mineral phase, thereby reducing the inevitability of localized junction failure.

Our fibril-level SEM studies included (a) regions of the still unruptured CEP-VEP junction, (b) ruptured regions where there is still an attached portion of the VEP bone, and (c) regions right at the tip of localized ruptures. A wide variety of fibril-level morphologies were revealed that indicated interconnectivity between these two structurally contrasting hard tissue zones. We also observed, albeit infrequently, actual structural disjunctions where the subbundle fibrils ended abruptly (see Fig. 9d). The slight gap associated with this disjunction may be real or simply a consequence of the tensile-induced elongation of the now demineralized endplate, resulting in a slight, noncatastrophic separation of the CEP and VEP locally.

There appeared to be no pattern of consistent and continuous rupture that was confined to the CEP-VEP junction; instead, the rupture path tended to deviate repeatedly away from the junction into the VEP. This could be a consequence of localized differences in strength of the junction arising from a variable presence or absence of the above noted disjunctions in different

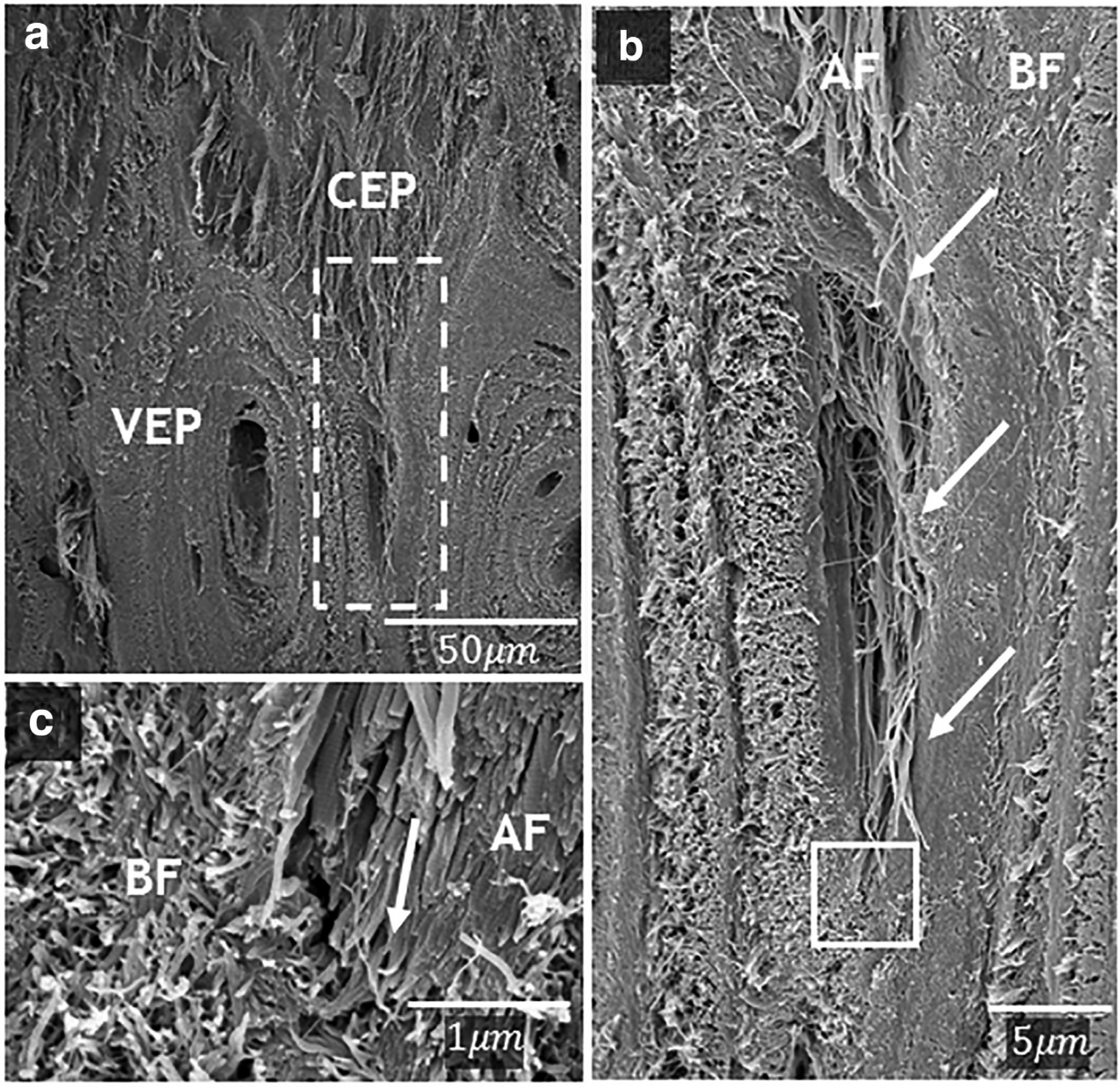

Fig. 5. Ultrastructural view of annular fibers (AF) extending deep in between osteons of the VEP at unruptured sites near the junction. (a) Low-magnification view. (b) Enlarged view of boxed region in (a) showing how the annular fibrils (AF) blend closely (see sites marked by white arrows) with the densely packed bony fibrils (BF) of the concentric osteon layers. (c) High magnification of the boxed region in (b) indicating what appears to be the termination of the AF on approaching the bony fibrils (BF) (see white arrow).

regions of the endplate. The sheer ambiguity of such rupture behavior again points to the CEP-VEP junction *not* being an inevitable zone of detachment in the healthy endplate complex.

Structurally, the overwhelming evidence from the SEM studies is that of an intimate intermingling and blending of the fibrils across the CEP-VEP junction and that no one morphology of interconnectivity prevails. Such fibril-level variability, combined with the fact that a full quota of matrix mineralization as demonstrated from the energy-dispersive X-ray spectroscopic analyses (see Fig. 3 and Table 1), renders the endplate junction region in the test control samples virtually failsafe compared to that of the mid-substance annulus or vertebral bone (see under *General* results section). This suggests to us a mechanism of composite reinforcement analogous to that exploited by structural engineers in their design of steel-reinforced concrete structures. In their design the engineer is coupling a high-strength tension-resisting element that has a significant degree of ductility (the steel) with a brittle material (the concrete), and one that is highly susceptible to failure in tension but strong in both compression and shear [19]. In

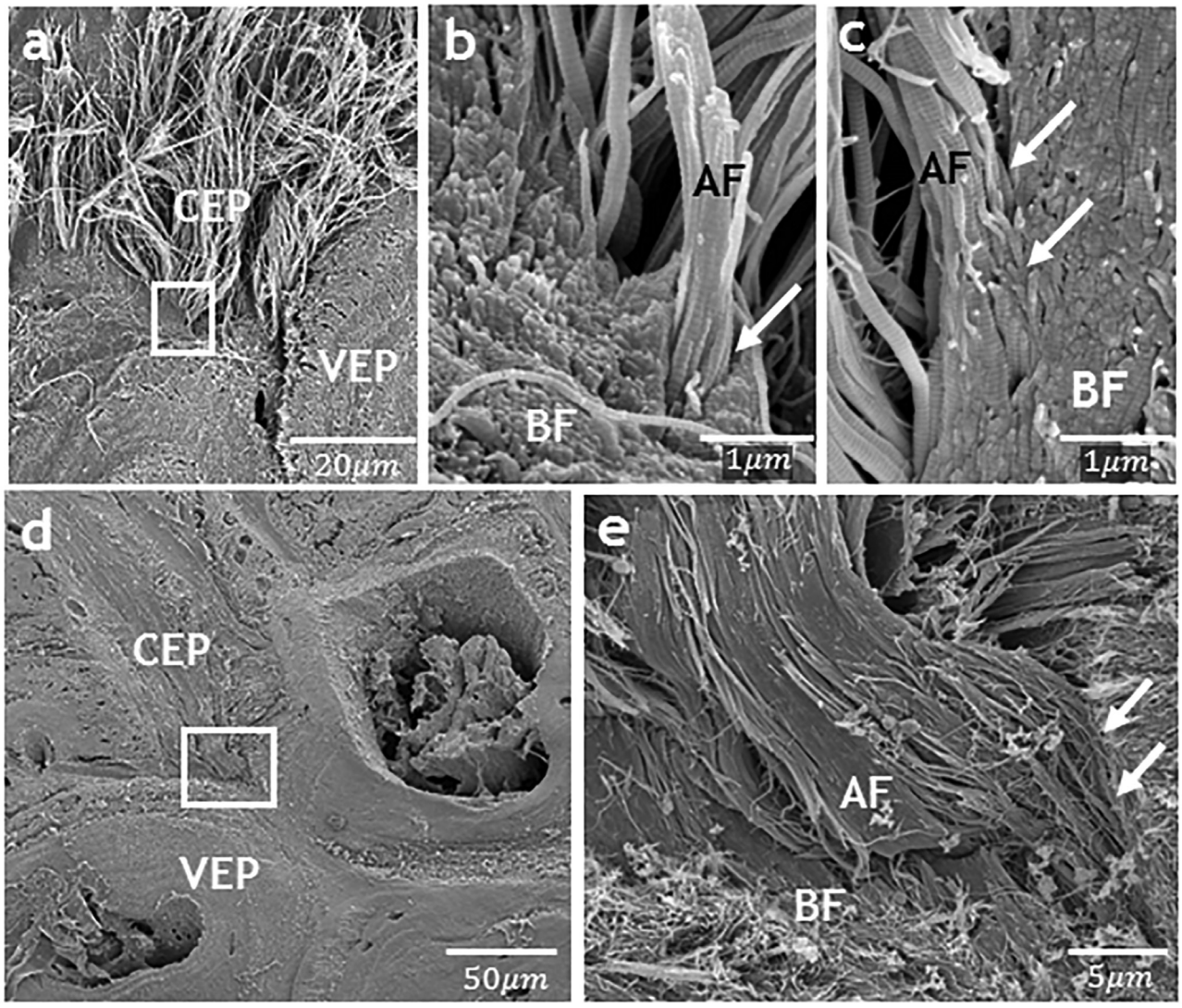

Fig. 6. Ultrastructural images of the CL showing how the annular fibrils (AF) merge or anchor into the bony fibrils (BF) at ruptured regions where there is still attached VEP bone. (a) A low-magnification image showing the junction between CEP and VEP. (b) Enlarged view of boxed region in (a) and showing clear evidence of anchoring of the AF bundles in the bony osteon fibrils (see white arrow). (c) Another example of AF anchoring and merging obliquely with the BF (see white arrows). (d) Low-magnification image showing annular bundles in the CEP inserting between two bony osteons of the VEP. (e) Enlargement of the boxed region in (d) showing a large annular bundle anchoring into the BF (see white arrows).

such structural systems, the various elements comprising the steelwork are brought into a close intermingling association but one that is not dependent on there being any direct bonding between them. The schematics in Fig. 10 provide three simple examples to illustrate key mechanisms that operate in such composite structures. The steel elements are, in fact, simply positioned in close proximity (in real life by via absurdly weak tie wires). It is then the concrete matrix that provides the all-important integrating medium [19].

The schematic in Fig. 10a illustrates how an effective tension-resisting linkage is created between separate load-bearing elements *without* them needing to be directly bonded; instead, the integrating mineral phase does this. In effect, tensile forces in one element are transferred into the other adjacent element via shear stresses carried by the bond created between each element and the embedding matrix, a mechanism referred as shear stress transfer in fiber-reinforced composite theory [20]. Fig. 10b and c illustrates how tensile forces applied to the steel reinforcing elements in different arrangements are also converted safely into compressive stresses within the brittle concrete matrix.

The following question then arises: could strengthening mechanisms similar to those discussed above for reinforced concrete also operate across the CEP-VEP junction and thus explain its strength? Before addressing this question, it is important to emphasize that these mechanisms rely on the steel and concrete components having a comparable degree of stiffness and for several important reasons as

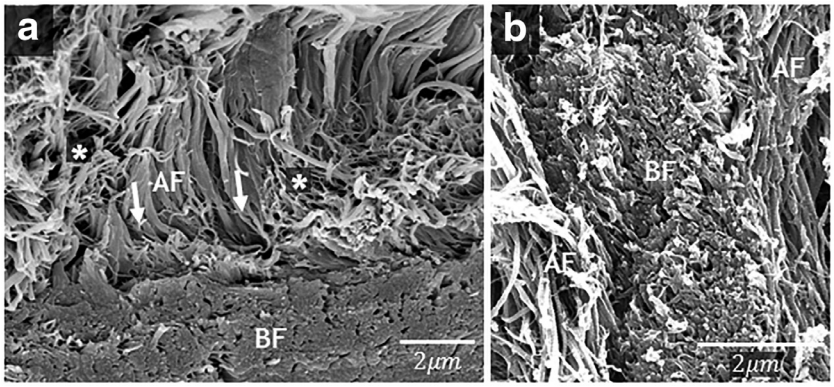

Fig. 7. (a) Image illustrating a method of integration across the still unruptured CEP-VEP junction involving a disorganized mass of bony fibrils (BF; see asterisks) that appear to act as a mediating zone between the annular fibrils (AF; see arrows) and more ordered fibrils of the osteons (BF). (b) Evidence of a more organized BF located in between two bundles of AF near the CL junction.

follows. Because the concrete is highly vulnerable to fracture under tensile loading conditions, the steel elements are positioned so as to protect the concrete from being exposed to such loading. However, the steel can only perform this protective role if there is a high degree of elastic strain compatibility between them, otherwise there would be extensive de-bonding between the steel and concrete, thereby exposing the concrete to dangerous tensile loads. It is the coupling between these two strain-matched components that allows such composite systems to be used so successfully in an enormous range of large-scale public structures.

But is there a comparable matching of elastic moduli between the mineral phase and the collagen fibrils comprising the endplate? Although the relatively low stiffness of the free collagen fibrils in the annular layers is fundamental to the disc functioning as a flexible link between adjacent

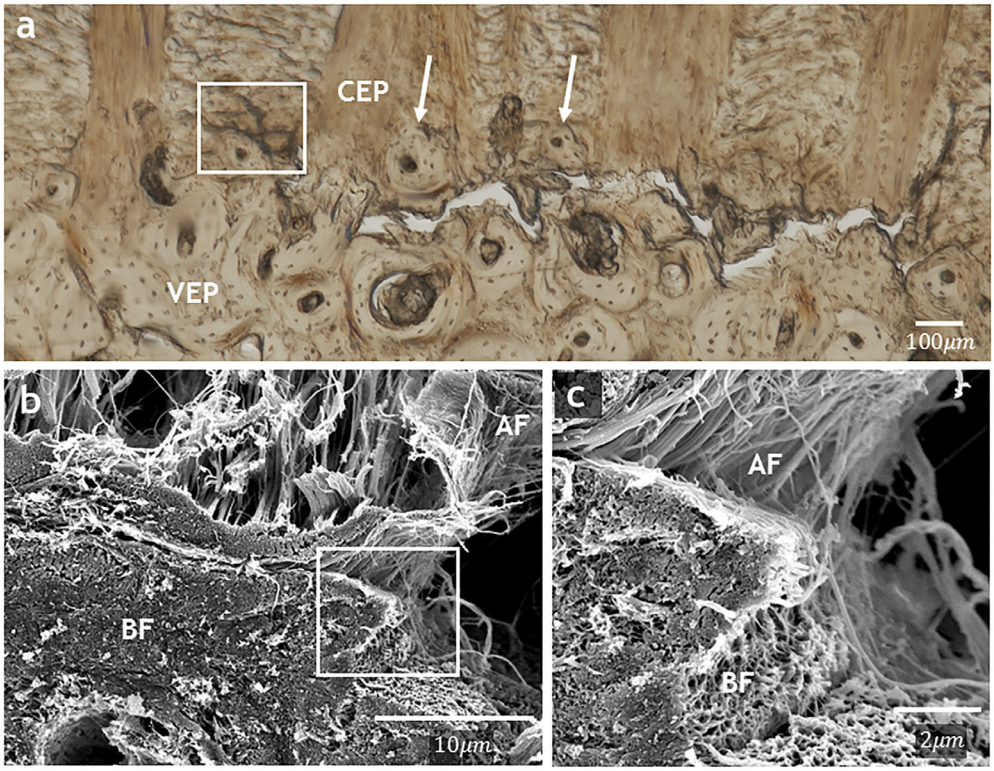

Fig. 8. Optical DIC and ultrastructural images of a sample that involved both partial CEP-VEP rupture and mid-substance failure. (a) DIC image showing osteon bone still attached to the now separated CEP as indicated by the white arrows. (b) Ultrastructural images of the boxed region in (a) showing counter oblique annular fibrils (AF) and the bony fibrils (BF) at the CL junction. (c) Enlarged view of the boxed region in (b) illustrating peeling of the annular subbundles (AF) from the bony matrix.

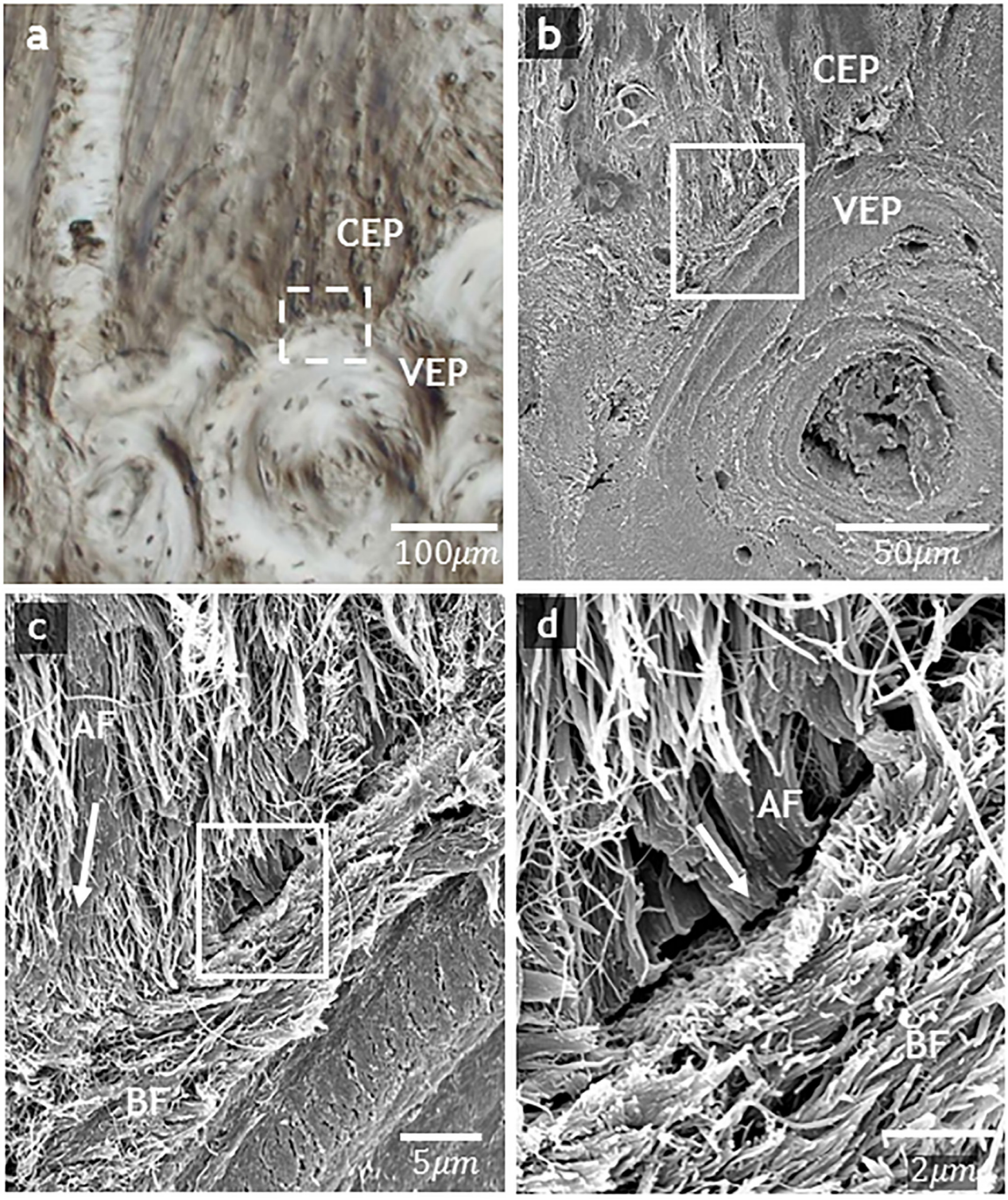

Fig. 9. (a) Optical DIC image of an unruptured region of CEP-VEP junction. (b) Low-magnification SEM image of the boxed region in (a). (c) Enlarged fibril-level view of the boxed region in (b) showing both the merging of annular and bony fibrils (see arrow) and annular fibrils that terminate abruptly without any apparent blending (see box). (d) Enlarged view of the boxed region in (c) illustrating both the abrupt termination of the annular fibers and a clear zone of separation.

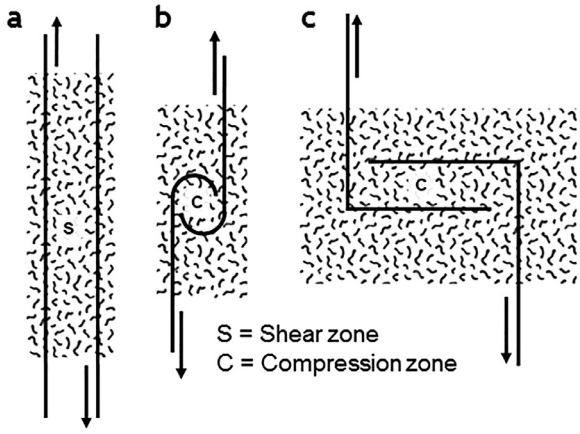

Fig. 10. Schematics illustrating how tensile forces carried by the steel elements are converted safely into either shear (see S) or compressive (see C) zone within the integrating concrete matrix.

stiff vertebrae, those fibrils in the calcified regions of the endplate have deposits of mineral *within* their hierarchical structure and thus will have a stiffness roughly comparable to that of the extrafibrillar mineral phase [21].

It therefore seems entirely plausible to argue that the CEP-VEP junction derives its strength in tension (as demonstrated in the present study) from mechanisms that approximate those known to operate in the steel-concrete system. Based on the various fibril-level SEM images in Figs. 5 to 9, the schematics in Fig. 11 offer a simplified representation of these and the mechanisms by which they might create a robust integration between the two distinct fibril sets comprising the CEP and VEP once mineralized.

The schematic in Fig. 11a models the annular fibrils penetrating deep in between the osteons layers, thus approximating the SEM images shown in Fig. 5. The schematic in

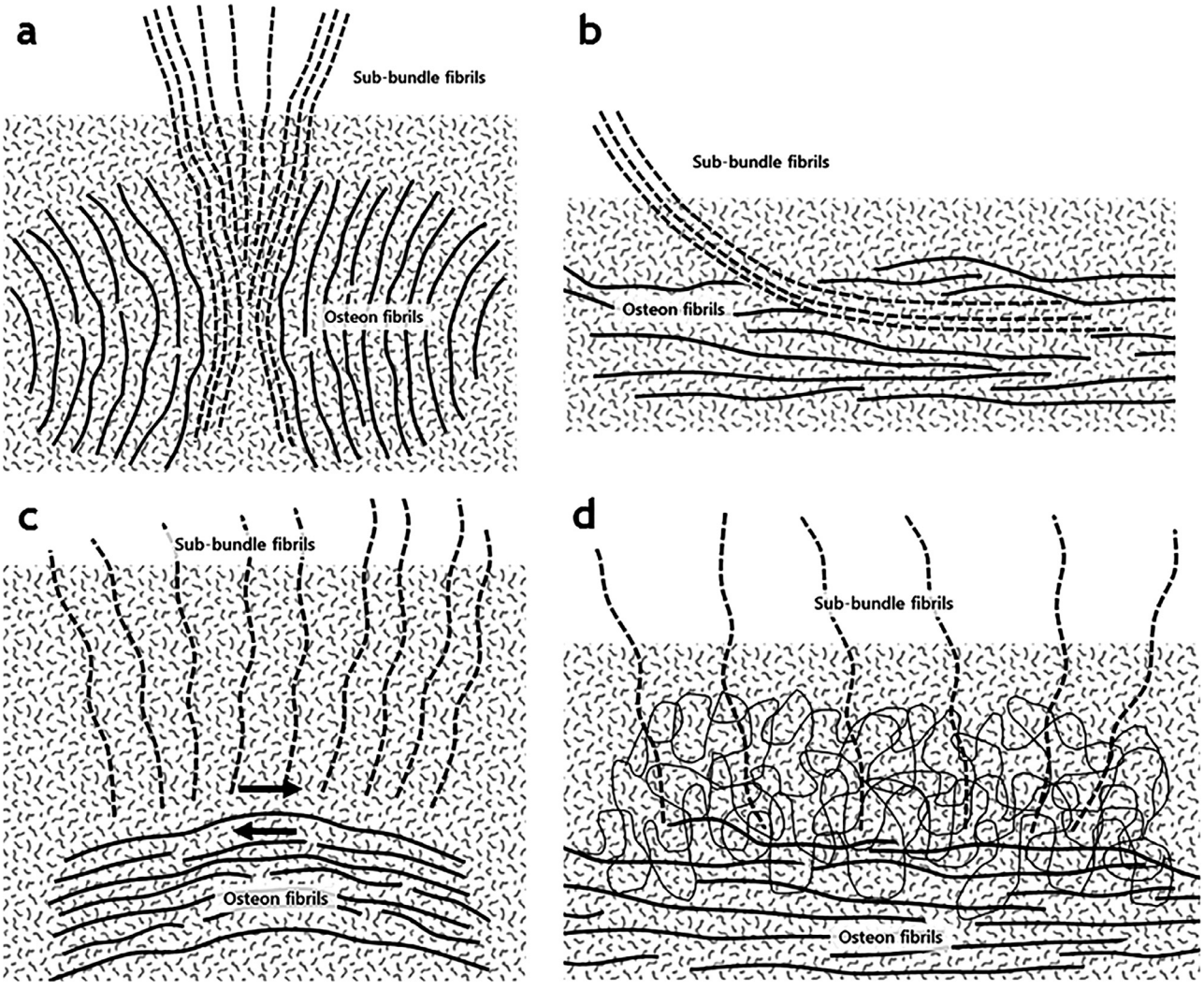

Fig. 11. Four generalized structural models based on the authors' morphological descriptions of fibril-level interaction across the CEP-VEP junction. In each schematic, the textured areas represent the integrating rigid mineral phase. (a) Annular subbundle fibrils inserting deep between the osteon fibrils to provide high resistance to annular bundle pull-out. (b) Oblique insertion of subbundles into the osteon. (c) Subbundles ending abruptly close to the osteon layers but not blending with them. This would provide high shear resistance (see arrows) in the mineralized gap in the plane of the CEP-VEP junction but low pull-out resistance. (d) Integration between the fibrils in the annular subbundles and fibril osteons is facilitated with an intervening irregular fibrillar network, which, once mineralized, would offer resistance to both annular pull-out and shear in the plane of junction.

Fig. 11b illustrates a direct but oblique insertion as suggested in the image set in Fig. 6a-e. Fig. 11c models the infrequently observed mineralized separation or gap as shown in Fig. 9d. This latter morphology would have a low subbundle pull out strength but a relatively high resistance to shear in the plane of the junction. Last, Fig. 11d illustrates the irregular array of intervening fibrils between the subbundle fibrils and the osteons as shown in Fig. 7, which, once mineralized, provides resistance to both pull-out and shear in the plane of the junction.

We have endeavored to describe the variety of fibril-level anchoring systems that can be identified in the CEP-VEP junction region. Of course, viewing this junction region at the level of the fibril presents to the electron microscopist an overwhelming amount of structural detail and we do not pretend to have included in the present study anything more than sufficient evidence to demonstrate that there is structural integration across the CEP-VEP junction in the ovine lumbar endplate system. This, in combination with mineralization, provides a structural basis for this region's mechanical robustness and is consistent with more recent studies that have reported a moderate frequency of human lumbar disc herniations with still-attached fragments of bone [3].

Limitations of study

First, our use of an ovine lumbar model obviously limits to some degree any comparison with the human equivalent. However, the ovine model does offer the advantage of a readily available source of healthy intervertebral discs that have many structural features in common with human discs and has been judged as offering a realistic model for investigating biomechanical principles relevant to the human disc [22–29]. There is also a considerable number of studies focusing on the structure of the ovine lumbar intervertebral discs that have demonstrated relevance to that of the human disc [6,7,30–34].

Another limitation concerns our use of fixation and demineralization prior to mechanical stretching in order to induce partial rupture. However, because we are not measuring actual strength values, we considered the method to be a legitimate means of creating partial rupture within the region of the junction. This in turn has enabled us to infer how mineralization interacts with the fibril structure in order to achieve CEP-VEP junction integration.

Conclusions

Using targeted decalcification of the endplate region and in-plane tensile loading to achieve incomplete rupture at the CL, this micro- and ultra-structural study reveals how the fibril-level structure is involved in the formation of this mechanically robust junction. Clear evidence of structural connectivity across the cartilaginous-vertebral endplate junction is observed with no single morphology of integration appearing to dominate. This is achieved by the intermingling of the fibrillar components and mediated by the mineral phase. These findings are consistent with clinical findings indicating, at times, the presence of not only cartilage but also attached bone fragments in herniated material.

Acknowledgement

Author NH Sapiee gratefully acknowledges Medtronic Australasia for funding her doctoral scholarship.

References

[1] Adams M, Bogduk N, Burton K, Dolan P. The biomechanics of back pain. 3rd ed. Edinburgh: Churchill Livingstone; 2013.
[2] Postacchini F. Lumbar disc herniation. Wein: Springer; 1999.
[3] Rajasekaran S, Bajaj N, Tubaki V, Kanna RM, Shetty AP. ISSLS Prize Winner: the anatomy of failure in lumbar disc herniation. Spine 2013;38:1491–500. doi: 10.1097/BRS.0b013e31829a6fa6.
[4] Lama P, Zehra U, Balkovec C, Claireaux HA, Flower L, Harding IJ, et al. Significance of cartilage endplate within herniated disc tissue. Eur Spine J 2014;23:1869–77. doi: 10.1007/s00586-014-3399-3.
[5] Sahoo MM, Mahapatra SK, Kaur S, Sarangi J, Mohapatra M. Significance of vertebral endplate failure in symptomatic lumbar disc herniation. Glob Spine J 2017;7:230–8. doi: 10.1177/2192568217694142.
[6] Rodrigues SA, Wade KR, Thambyah A, Broom ND. Micromechanics of annulus–end plate integration in the intervertebral disc. Spine J 2012;12:143–50. doi: 10.1016/j.spinee.2012.01.003.
[7] Rodrigues SA, Thambyah A, Broom ND. A multiscale structural investigation of the annulus-endplate anchorage system and its mechanisms of failure. Spine J 2015;15:405–16. doi: 10.1016/j.spinee.2014.12.144.
[8] Junhui L, Zhengfeng M, Zhi S, Mamuti M, Lu H, Shunwu F, et al. Anchorage of annulus fibrosus within the vertebral endplate with reference to disc herniation. Microsc Res Tech 2015;78:754–60. doi: 10.1002/jemt.22536.
[9] Humzah MD, Soames RW. Human intervertebral disc: Structure and function. Anatom Rec 1988;220:337–56. doi: 10.1002/ar.1092200402.
[10] Berg-Johansen B, Fields AJ, Liebenberg EC, Li A, Lotz JC. Structure-function relationships at the human spinal disc-vertebra interface. J Orthop Res 2017;36:1–10. doi: 10.1002/jor.23627.
[11] Brown S, Rodrigues S, Sharp C, Wade K, Broom N, McCall IW, et al. Staying connected: structural integration at the intervertebral disc-vertebra interface of human lumbar spines. Eur Spine J 2016;26:248–58. doi: 10.1007/s00586-016-4560-y.
[12] Balkovec C, Adams MA, Dolan P, McGill SM. Annulus fibrosus can strip hyaline cartilage end plate from subchondral bone: a study of the intervertebral disk in tension. Glob Spine J 2015;5:360–5. doi: 10.1055/s-0035-1546956.
[13] Inoue H. Three-dimensional architecture of lumbar intervertebral discs. Spine 1978;6:139–46. PMID: 7280814.
[14] Roberts S, Menage J, Urban JPG. Biochemical and structural properties of the cartilage end-plate and its relation to the intervertebral disc. Spine 1988;14:166–74.
[15] Vernon-Roberts B, Moore RJ, Fraser RD. The natural history of age-related disc degeneration: the pathology and sequelae of tears. Spine 2007;32:2797–804. doi: 10.1097/BRS.0b013e31815b64d2.
[16] Sinclair SK, Bell S, Epperson RT, Bloebaum RD. The significance of calcified fibrocartilage on the cortical endplate of the translational sheep spine model. Anatom Rec 2013;296:736–44. doi: 10.1002/ar.22683.
[17] Paietta RC, Burger EL, Ferguson VL. Mineralization and collagen orientation throughout aging at the vertebral endplate in the human

lumbar spine. J Struct Biol 2013;184:310–20. doi: 10.1016/j.jsb.2013.08.011.
[18] Gupta HS, Schratter S, Tesch W, Roschger P, Berzlanovich A, Schoeberl T, et al. Two different correlations between nanoindentation modulus and mineral content in the bone-cartilage interface. J Struct Biol 2005;149:138–48. doi: 10.1016/j.jsb.2004.10.010.
[19] Nawy EG. Reinforced concrete: a fundamental approach. 6th ed.. Upper Saddle River, NJ: Pearson; 2009. chaps. 4 and 10.
[20] Caddell RM. Deformation and fracture of solids. Englewood Cliffs, NJ: Prentice-Hall; 1980. p. 252–71.
[21] Weiner S, Wagner HD. The material bone: structure-mechanical function relations. Annu Rev Mater Sci 1998;28:271–98. doi: 10.1146/annurev.matsci.28.1.271.
[22] Alini M, Eisenstein SM, Ito K, Little C, Kettler AA, Masuda K, et al. Are animal models useful for studying human disc disorders/degeneration? Eur Spine J 2008;17:2–19. doi: 10.1007/s00586-007-0414-y.
[23] Wilke HJ, Kettler A, Wenger KH, Claes LE. Anatomy of the sheep spine and its comparison to the human spine. Anatom Rec 1997;247:542–55. doi: 10.1002/(SICI)1097-0185(199704)247:4<542::AID-AR13>3.0.CO;2-P.
[24] Lotz JC. Animal models of intervertebral disc degeneration lessons learned. Spine 2004;29:2742–50. doi: 10.1097/01.brs.0000146498.04628.f9.
[25] Sheng SR, Wang XY, Xu HZ, Zhu GQ, Zhou YF. Anatomy of large animal spines and its comparison to the human spine: a systematic review. Eur Spine J 2010;19:46–56. doi: 10.1007/s00586-009-1192-5.
[26] Wilke H-J, Kettler A, Claes LE. Are sheep spines a valid biomechanical model for human spines? Spine 1997;22:2365–74. doi: 10.1097/00007632-199710150-00009.
[27] Reid JE, Meakin JR, Robins SP, Skakle JMS, Hukins DWL. Sheep lumbar intervertebral discs as models for human discs. Clin Biomech 2002;17:312–4. doi: 10.1016/S0268-0033(02)00009-8.
[28] Easley NE, Wang M, McGrady LM, Toth JM. Biomechanical and radiographic evaluation of an ovine model for the human lumbar spine. Proc Inst Mech Eng, Part H: J Eng Med 2008;222:915–22. doi: 10.1243/09544119JEIM345.
[29] Schollum ML, Robertson PA, Broom ND. A microstructural investigation of intervertebral disc lamellar connectivity: detailed analysis of the translamellar bridges. J Anat 2009;214:805–16. doi: 10.1111/j.1469-7580.2009.01076.x.
[30] Schollum ML, Robertson PA, Broom ND. ISSLS Prize Winner: microstructure and mechanical disruption of the lumbar disc annulus. Spine 2008;33:2702–10. doi: 10.1097/BRS.0b013e31817bb92c.
[31] Wade KR, Robertson PA, Broom ND. A fresh look at the nucleus-endplate region: new evidence for significant structural integration. Eur Spine J 2011;20:1225–32. doi: 10.1007/s00586-011-1704-y.
[32] Wade KR, Robertson PA, Broom ND. Influence of maturity on nucleus-endplate integration in the ovine lumbar spine. Eur Spine J 2014;23:732–44. doi: 10.1007/s00586-014-3181-6.
[33] Wade KR, Robertson PA, Broom ND. On the extent and nature of nucleus-annulus integration. Spine 2012;37:1826–33. doi: 10.1097/BRS.0b013e3182637f04.
[34] Wade KR, Robertson PA, Broom ND. On how nucleus-endplate integration is achieved at the fibrillar level in the ovine lumbar disc. J Anat 2012;221:39–46. doi: 10.1111/j.1469-7580.2012.01507.x.